PROCEEDINGS OF SCIENCE

Autocorrelation studies in two-flavour Wilson Lattice QCD using DD-HMC algorithm

Abhishek Chowdhury[a], **Asit K. De**[a], **Sangita De Sarkar**[a], **A. Harindranath**[a], **Jyotirmoy Maiti**[b], **Santanu Mondal**[*a], **Anwesa Sarkar**[a]

[a]*Theory Division, Saha Institute of Nuclear Physics*
1/AF Bidhan Nagar, Kolkata 700064, India
[b]*Department of Physics, Barasat Government College,*
10 KNC Road, Barasat, Kolkata 700124, India

E-mail: santanu.mondal@saha.ac.in

We perform an extensive study of autocorrelation of several observables in lattice QCD with two degenerate flavours of naive Wilson fermions using DD-HMC algorithm and show that (1) at a given lattice spacing, autocorrelations of topological susceptibility and pion and nucleon propagators with wall source decrease with decreasing quark mass, (2) autocorrelation of topological susceptibility substantially increases with decreasing lattice spacing but autocorrelation of topological charge density correlator shows only mild increase and (3) increasing the size and the smearing level increase the autocorrelation of Wilson loop.

The 30th International Symposium on Lattice Field Theory
June 24 - 29, 2012
Cairns, Australia

*Speaker.

PoS(Lattice 2012)189

1. Introduction

The most popular algorithm to simulate lattice QCD with dynamical fermions is the Hybrid Monte Carlo (HMC) [1] and one of its improved variations, namely, Domain Decomposed Hybrid Monte Carlo (DD-HMC) [2] aims to achieve significant acceleration of the numerical simulation. Dynamical Wilson fermion simulations at smaller quark masses, smaller lattice spacings and larger lattice volumes on currently available computers have become feasible with recent developments such as DD-HMC algorithm. However, approach to the continuum and chiral limits may still be hampered by the phenomenon of critical slowing down. One of the manifestation of critical slowing down is the increase in autocorrelation times associated with the measurements of various observables. Thus measurements of autocorrelation times help us to evaluate the performance of an algorithm in overcoming critical slowing down. In addition, an accurate determination of the uncertainty associated with the measurement of an observable requires a realistic estimation of the autocorrelation of the observable which in turn depends on the various parameters associated with the particular algorithm used.

An extensive study of autocorrelation mainly in pure gauge theory has been carried out by ALPHA collaboration [3]. They have shown that the autocorrelation of squared topological charge increases dramatically with decreasing lattice spacing while Wilson loops decouple from the modes which slow down the topological charge as lattice spacing decreases. In the simulations with dynamical fermions, the study becomes more difficult because the autocorrelation may now depend on number of quark flavours (n_f), the quark masses and the fermion action used [4]. In this work we study the autocorrelations of a variety of observables measured with DD-HMC algorithm in the case of naive Wilson fermions [5, 6]. Note that the measurement of autocorrelation is notoriously difficult, since accurate determination of it may require considerably longer trajectories. In this work we mainly focus on various trends of autocorrelations that we can observe clearly rather than the precise measurement of the integrated autocorrelation time.

2. Autocorrelation

The unnormalized autocorrelation function,

$$C^{\mathscr{O}}(t) = \langle \mathscr{O}(s)\mathscr{O}(s+t)\rangle - \mu_{\mathscr{O}}^2 \tag{2.1}$$

where $\mu_{\mathscr{O}} \equiv \langle \mathscr{O}(t)\rangle$. Now if the algorithm satisfies detailed balance and ergodicity, following Refs. [3] and [7] one can arrive at, $C^{\mathscr{O}}(t) = \sum_{n\geq 1} e^{-t/\tau_n} \mid \eta_n(\mathscr{O}) \mid^2$ where $\tau_n = -\frac{1}{\ln \lambda_n}$, assuming λ_n's, eigenvalues of symmetrized transition matrix are positive.

For any particular observable $\mathscr{O}$, autocorrelation among the generated configurations are generally determined by the integrated autocorrelation time $\tau_{\text{int}}^{\mathscr{O}}$ for that observable. For this purpose, at first, one needs to calculate the unnormalized autocorrelation function of the observable $\mathscr{O}$ measured on a sequence of N equilibrated configurations as

$$C^{\mathscr{O}}(t) = \frac{1}{N-t}\sum_{r=1}^{N-t}\left(\mathscr{O}_r - \overline{\mathscr{O}}\right)\left(\mathscr{O}_{r+t} - \overline{\mathscr{O}}\right) \tag{2.2}$$

where $\overline{\mathscr{O}} = \frac{1}{N}\sum_{r=1}^{N}\mathscr{O}_r$ is the ensemble average. Following the *windowing* method as recommended by Ref. [7], the integrated autocorrelation time is defined as

$$\tau_{\rm int}^{\mathscr{O}} = \frac{1}{2} + \sum_{t=1}^{\rm W}\Gamma^{\mathscr{O}}(t) \tag{2.3}$$

where $\Gamma^{\mathscr{O}}(t) = C^{\mathscr{O}}(t)/C^{\mathscr{O}}(0)$ is the normalized autocorrelation function and W is the summation window. The errors are calculated by the single omission jackknife method.

3. Observables

Let us denote plaquette and Wilson loop of size $R \times T$ with HYP smear level s by P_s and $W_s(R,T)$ respectively. Topological susceptibility with smear level s is denoted by Q_s^2 (the normalization factor, inverse of lattice volume, is ignored). We have measured the autocorrelations for the plaquette, Wilson loop, nucleon propagator, pion propagator, topological susceptibility and topological charge density correlator ($C(r) = \langle q(x)q(0)\rangle$ where $q(x)$ is topological charge density and $r = \mid x \mid$) for the saved configurations except for the unsmeared plaquette where we have measured for all the configurations, at two values of gauge coupling ($\beta = 5.6$ and 5.8) and several values of the hopping parameter κ. Our notations and conventions used for pion and nucleon observables are given in Ref. [8]. We measure the autocorrelation of the zero spatial momentum correlation functions at an appropriate time slice corresponding to the plateau region of the effective mass. For lattice volume $24^3 \times 48$ and $32^3 \times 64$ we use 12^{th} and 15^{th} time slices respectively. Our data for topological charge, susceptibility and charge density correlator are presented in [10, 11, 12].

4. Auto-correlation Measurements

We have generated ensembles of gauge configurations by means of DD-HMC [2] algorithm using unimproved Wilson fermion and gauge actions [5, 6] with $n_f = 2$ mass degenerate quark flavors. At $\beta = 5.6$ the lattice volumes are $24^3 \times 48$ and $32^3 \times 64$ and the renormalized physical quark mass (calculated using axial Ward identity) ranges between 25 to 125 MeV ($\overline{\rm MS}$ scheme at 2 GeV). At $\beta = 5.8$ the lattice volume is $32^3 \times 64$ and the renormalized physical quark mass ranges from 15 to 75 MeV ($\overline{\rm MS}$ scheme at 2 GeV). The lattice spacings are determined using nucleon mass to pion mass ratio and Sommer method. These determinations agree for the value of Sommer parameter $r_0 = 0.44$ fm. The lattice spacings at $\beta = 5.6$ and 5.8 are 0.069 and 0.053 fm respectively. The number of thermalized configurations ranges from 7000 to 14000 and the number of measured configurations ranges from 150 to 2000. For the lattice parameters and simulation statistics see [8] . For all ensembles of configurations the average Metropolis acceptance rates range between 75-98%.

5. Results

Fig. 1 shows that for two lattice spacings ($\beta = 5.6, 5.8$) autocorrelations of Q_{20}^2 decrease with decreasing quark mass even though for the smaller quark mass at $\beta = 5.8$ ($\kappa = 0.15475$)

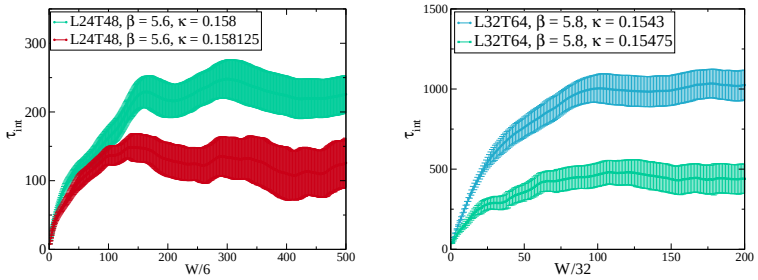

Figure 1: Integrated autocorrelation times for topological susceptibilities (Q^2_{20}) at $\beta = 5.6$ ($a = 0.069$ fm) (left) and at $\beta = 5.8$ (right) ($a = 0.053$ fm).

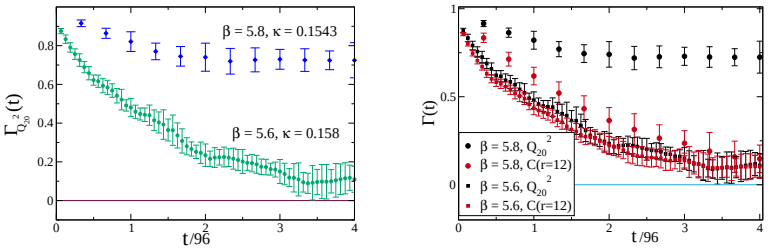

Figure 2: Comparison of normalized autocorrelation functions for Q^2_{20} (left) and Q^2_{20}, $C(r = 12.0)$ (right) at $\beta = 5.6$, $\kappa = 0.158$ and $\beta = 5.8$, $\kappa = 0.1543$ with lattice volumes $24^3 \times 48$ and $32^3 \times 64$ respectively.

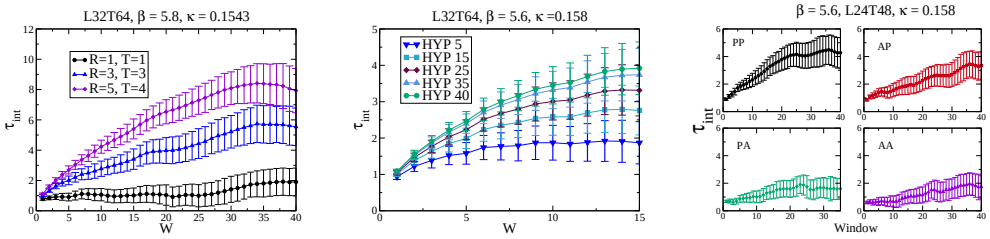

Figure 3: Integrated autocorrelation times of Wilson loops for different sizes (left) and for different levels of HYP smearing (middle). Integrated autocorrelation times for *PP*, *AP*, *PA* and *AA* correlators with wall source, measurements are done with a gap of 24 trajectories (right).

molecular dynamics trajectory length is smaller. A possible explanation [1] for this suppression of autocorrelation with decreasing quark mass is that the algorithm needs to span between lesser number of topological sectors at smaller quark mass since the width of the Gaussian distribution of topological charge decreases with decreasing quark mass.

Fig. 2 shows that autocorrelation for Q^2_{20} increases quite significantly with decreasing lattice spacing at comparable quark mass whereas the autocorrelation of $C(r)$ (Fig. 2 (right)) increases slightly with decreasing lattice spacing.

For the measurement of static potential $V(r)$ one needs to measure Wilson loops of various

[1] Stefan Schaefer (private communication)

$\beta = 5.6$

κ	*lattice*	*block*	τ_{int}^{Pion}	$\tau_{int}^{Nucleon}$
0.158	$24^3 \times 48$	$6^3 \times 8$	99(19)	75(18)
0.158125	$24^3 \times 48$	$6^3 \times 8$	50(9)	34(9)
0.15825	$24^3 \times 48$	$6^3 \times 8$	40(10)	25(9)
0.158	$32^3 \times 64$	$8^3 \times 16$	39(13)	33(17)
0.15815	$32^3 \times 64$	$8^3 \times 16$	31(15)	26(7)
0.15825	$32^3 \times 64$	$8^3 \times 16$	34(11)	18(6)

Table 1: Integrated autocorrelation times for pion (*PP*) and nucleon propagators with wall sources at $\beta = 5.6$. Here *block* refers to DD-HMC block.

sizes. In the measurement of a Wilson loop, to suppress unwanted fluctuations smearing is needed. Therefore it is interesting to study how autocorrelation of Wilson loops changes with sizes of the Wilson loops and smearing levels. In Fig. 3 we present integrated autocorrelation times for W_{20} with different sizes (left) and $W(4,4)$ with different levels of HYP smearing (middle). We observe that the integrated autocorrelation time increases with the increasing size of the Wilson loop and also with the increasing smearing level. In the context of Wilson loop and Polyakov loop, SESAM collaboration has observed that geometrically extended observables suffer more from autocorrelation [13].

In the following discussion P, A denote pseudoscalar and fourth component of axial vector densities respectively. In Table 1 integrated autocorrelation times for pion (PP) and nucleon propagators with wall sources at a given time slice are presented. Clearly the integrated autocorrelation time decreases with increasing κ both for pion and nucleon propagators. Similar observation was made by ALPHA collaboration in the case of Clover fermion [14]. The autocorrelation times of pion and nucleon propagators with point source and sink are smaller than the gap with which configurations are saved. For the determination of pion decay constants and PCAC quark mass, pion propagators other than PP are also needed. In Fig. 3 (right) the integrated autocorrelation times for PP, AP, PA and AA correlators with wall source for at $\beta = 5.6$, $\kappa = 0.158$ and lattice volume $24^3 \times 48$ are presented. The propagators with A in the source are less correlated than P in the source.

6. Improved estimation of τ_{int}

Following Ref. [3], an improved estimation of $\tau_{\rm int}$ can be determined as follows. Let τ^* be the best estimate of the dominant time constant. If for an observable $\mathscr{O}$ all relevant time scales are smaller or of the same order of τ^* then the upper bound of $\tau_{\rm int}$

$$\tau_{\rm int}^{u} \;=\; \frac{1}{2} \;+\Sigma_{t=1}^{W_u}\Gamma^{\mathscr{O}}(t)+A_{\mathscr{O}}(W_u)\;\tau^* \tag{6.1}$$

where $A_{\mathscr{O}} = \max(\Gamma^{\mathscr{O}}(W_u), 2\delta\Gamma^{\mathscr{O}}(W_u))$. W_u is chosen where the autocorrelation is still significant. One possible estimation of τ^* is by measuring effective autocorrelation time, which is introduced in

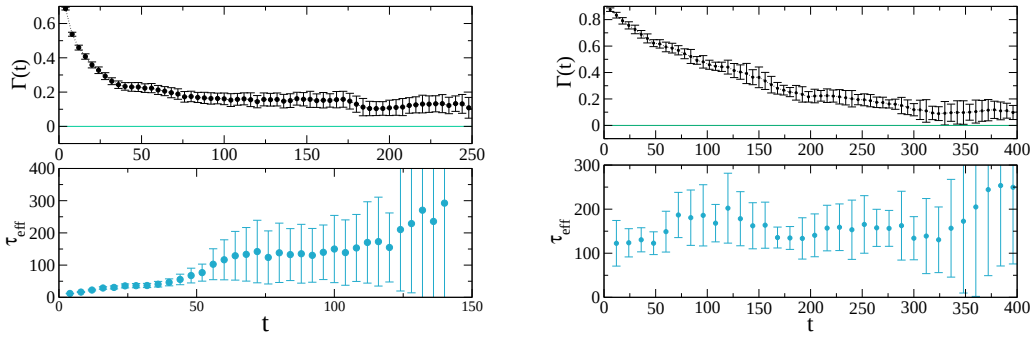

Figure 4: Normalized autocorrelation function and effective autocorrelation time for P_0 (left) Q^2_{20} (right) at $\beta = 5.6$, $\kappa = 0.158$ and lattice volume $24^3 \times 48$.

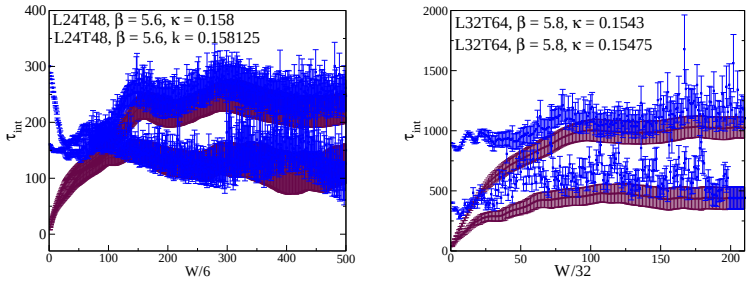

Figure 5: Integrated autocorrelation times and their upper bounds (τ^u_{int}) for topological susceptibilities (Q^2_{20}) at $\beta = 5.6$ ($a = 0.069$ fm) (left) and at $\beta = 5.8$ (right) ($a = 0.053$ fm).

Ref. [3] as described below. Define effective exponential autocorrelation time $\tau^{exp}_{eff}(\mathcal{O}) = \frac{t}{2\ln\frac{\Gamma^{\mathcal{O}}(t/2)}{\Gamma^{\mathcal{O}}(t)}}$. τ^{exp}_{eff} which can be an estimate of τ^* is defined as, $\tau^{exp}_{eff} = Max_{\mathcal{O}}[\frac{t}{2\ln\frac{\Gamma^{\mathcal{O}}(t/2)}{\Gamma^{\mathcal{O}}(t)}}]$. The estimation of $\tau^{exp}_{eff}(\mathcal{O})$ requires good signal to noise ratio in the asymptotic region in a case by case basis which in turn requires very long Markov chain and is beyond the scope of the present work.

However it is interesting to look at $\tau^{exp}_{eff}(\mathcal{O})$ where reliable data is available and we present such an example in Fig. 4 (the jackknife technique is used to calculate the error of $\tau^{exp}_{eff}(\mathcal{O})$). In Fig. 4 it appears that Q^2_{20} is coupling dominantly with slow mode, whereas P_0 is coupling with more than one modes; nevertheless the slowest mode appearing in P_0 is approximately the same as in Q^2_{20}. This is reflected in the behaviour of $\tau^{exp}_{eff}(\mathcal{O})$, which shows a single plateau for Q^2_{20}, but for P_0, there is more than one plateau and the data is more noisy. Similar behaviour is observed in pure gauge theory in Ref. [3].

In Fig. 5 we present the integrated autocorrelation times and their upper bounds (τ^u_{int}) for topological susceptibilities (Q^2_{20}) at $\beta = 5.6$ (left) and at $\beta = 5.8$ (right). At both lattice spacings, we find that both $\tau_{int}(Q^2_{20})$ and $\tau^u_{int}(Q^2_{20})$ decrease as quark mass decreases.

In conclusion, an extensive study of autocorrelation of several observables in lattice QCD with two degenerate flavours of naive Wilson fermion has shown that (1) at a given lattice spacing,

autocorrelations of topological susceptibility and pion and nucleon propagators with wall source decrease with decreasing quark mass, (2) autocorrelation of topological susceptibility substantially increases with decreasing lattice spacing but autocorrelation of topological charge density correlator shows only mild increase and (3) increasing the size and the smearing level increase the autocorrelation of Wilson loop.

Acknowledgements

Numerical calculations are carried out on Cray XD1 and Cray XT5 systems supported by the 10th and 11th Five Year Plan Projects of the Theory Division, SINP under the DAE, Govt. of India. We thank Richard Chang for the prompt maintenance of the systems and the help in data management. This work was in part based on the public lattice gauge theory codes of the MILC collaboration [9] and Martin Lüscher [2].

References

[1] S. Duane, A. D. Kennedy, B. J. Pendleton, D. Roweth, Phys. Lett. **B195**, 216 (1987).

[2] M. Lüscher, Comput. Phys. Commun. **156**, 209-220 (2004). [hep-lat/0310048]; M. Lüscher, Comput. Phys. Commun. **165**, 199-220 (2005). [hep-lat/0409106].
`http://luscher.web.cern.ch/luscher/DD-HMC/index.html`

[3] S. Schaefer *et al.* [ALPHA Collaboration], Nucl. Phys. B **845**, 93 (2011) [arXiv:1009.5228 [hep-lat]].

[4] M. Luscher, PoS LATTICE **2010**, 015 (2010) [arXiv:1009.5877 [hep-lat]].

[5] K. G. Wilson, Phys. Rev. **D10**, 2445-2459 (1974).

[6] K. G. Wilson, "Quarks and Strings on a Lattice", in *New Phenomena in Subnuclear Physics*, Proceedings of the International School of Subnuclear Physics, Erice, 1975, edited by A. Zichichi (Plenum, New York, 1977).

[7] N. Madras and A. D. Sokal, J. Stat. Phys. **50**, 109 (1988); A. D. Sokal, *Monte Carlo Methods in Statistical Mechanics: Foundations and New Algorithms*, NATO Adv. Sci. Inst. Ser. B Phys., Vol. 361, Plenum, New York, (1997), pp. 131-192.

[8] A. Chowdhury, A. K. De, S. De Sarkar, A. Harindranath, J. Maiti, S. Mondal and A. Sarkar, arXiv:1209.3915 [hep-lat].

[9] `http://physics.indiana.edu/~sg/milc.html`

[10] A. Chowdhury, A. K. De, S. De Sarkar, A. Harindranath, S. Mondal, A. Sarkar and J. Maiti, Phys. Lett. B **707**, 228 (2012) [arXiv:1110.6013 [hep-lat]].

[11] A. Chowdhury, A. K. De, S. De Sarkar, A. Harindranath, S. Mondal, A. Sarkar and J. Maiti, PoS LATTICE **2011**, 099 (2011) [arXiv:1111.1812 [hep-lat]].

[12] A. Chowdhury, A. K. De, A. Harindranath, J. Maiti and S. Mondal, "Topological charge density correlator in Lattice QCD with two flavours of unimproved Wilson fermions", arXiv:1208.4235v1 [hep-lat].

[13] Th. Lippert et.al. Nucl. Phys. Proc. Suppl. **60A**, 311 (1998) [hep-lat/9707004].

[14] M. Marinkovic, S. Schaefer, R. Sommer and F. Virotta, arXiv:1112.4163 [hep-lat].